

# Synthesis and Properties of Alkoxyethyl $\beta$ -D-Xylopyranoside

Wangzhen Shen<sup>1</sup> · Shanwei Ji<sup>1</sup> · Langqiu Chen<sup>1</sup> · Yanhua Zhang<sup>1</sup> · Xiubing Wu<sup>1</sup>

Received: 7 May 2017 / Revised: 13 August 2017 / Accepted: 26 October 2017  
© 2018 AOCS

**Abstract** In order to improve the water solubility of sugar-based surfactants, alkyl  $\beta$ -D-xylopyranosides, novel sugar-based surfactants, 1,2-trans alkoxyethyl  $\beta$ -D-xylopyranosides, with alkyl chain length  $n = 6$ –12 were stereoselectively prepared by the trichloroacetimidate method. Their properties including hydrophilic–lipophilic balance (HLB) number, water solubility, surface tension, emulsification, foamability, thermotropic liquid crystal, and hygroscopicity were investigated. The results indicated that their HLB number decreased with increase of alkyl chain, the water solubility improved since the hydrophilic oxyethene ( $-\text{OCH}_2\text{CH}_2-$ ) fragment was introduced. The dissolution process was entropy driven at 25–45 °C for alkyl chain length  $n = 6$ –10. Octyloxyethyl  $\beta$ -D-xylopyranoside had the best foaming ability. Nonyloxyethyl  $\beta$ -D-xylopyranoside had the best foam stability and the emulsifying ability was better in toluene/water system than in rapeseed oil/water system. The surface tension of in aqueous solution dropped to 27.8 mN m<sup>-1</sup> at the critical micelle concentration, and it also showed the most distinct thermotropic liquid phases with cross pattern texture upon heating and the fan schlieren texture on cooling. Hexyloxyethyl  $\beta$ -D-xylopyranoside possessed the strongest hygroscopicity. Based on the effective improvement of water solubility, the prepared

alkoxyethyl  $\beta$ -D-xylopyranosides showed excellent surface activity and are expected to develop their practical application as a class of novel sugar-based surfactants.

**Keywords** Surface activity · Synthesis · Non-ionic surfactants · Interfacial science

*J Surfact Deterg* (2018).

## Introduction

From a long-term point of view, shortage of petroleum resources will become more and more serious. Fortunately for our planet, there are solutions involving utilization of renewable materials and/or effective access to biodegradable products. A few surfactants are prepared from renewable materials and have excellent biodegradable properties. Alkyl polyglycosides (APGs) are safe and environmentally friendly sugar-based nonionic surfactants. APG is synthesized from carbohydrates and fatty alcohols that are naturally occurring and renewable raw materials (Ríos, Fernández-Arteaga, Lechuga, Jurado, & Fernández-Serrano, 2016). They have been employed in industrial and consumer application fields, such as detergents, food products, pharmaceuticals, agrochemicals, protein science, and personal care products, because they possess the excellent properties including low surface tension, efficient decontamination ability, exquisite and stable foam, low toxicity, and so on (Ardolino, Meloni, Brugali, Corsini, & Galli, 2016; Du, Wang, Tai, Wang, & Liu, 2016; Lukic, Pantelic, & Savic, 2016; Reading et al., 2015).

APG has a hydrophilic head group portion and a hydrophobic tail portion. The hydrophilic head group could be designated as glucosyl, galactosyl, maltosyl, xylosyl, and other glycosyl fragments (Baâzaoui et al., 2016; Bayach,

**Electronic supplementary material** The online version of this article (doi:10.1002/jsde.12013) contains supplementary material including syntheses, characterization and <sup>1</sup>H NMR spectra of target compounds (**6a–6f**), which is available to authorized users.

✉ Langqiu Chen  
chengood2003@263.net

<sup>1</sup> College of Chemistry, Key Laboratory of Environmentally Friendly Chemistry and Application of Ministry of Education, Xiangtan University, Xiangtan, 411105, Hunan, China

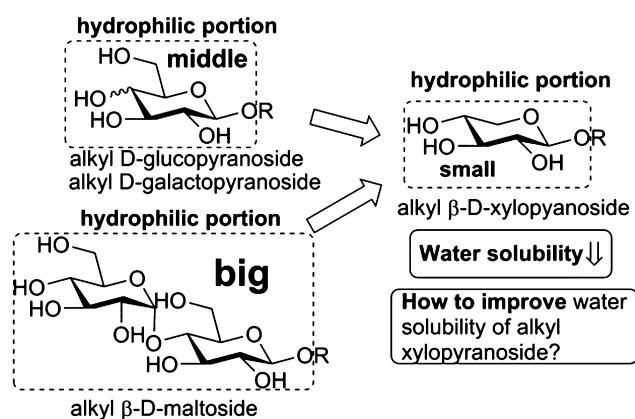


**Fig. 1** Water solubility of alkyl glycoside

Manickam-Achari, Iskandar, Sugimura, & Hashim, 2016; Charoensapyanan, Ito, Rudeekulthamrong, & Kaulpiboon, 2016; Chen, Li, Chen, Ji, & Shen, 2016; Guo, Xu, Kang, Han, & Zheng, 2016; Xu et al., 2012). The hydrophobic hydrocarbon tail group is usually composed of different chain lengths of saturated, fluorinated, or unsaturated alcohol (Chen, Li, et al., 2016; Xu et al., 2012). The most readily available monosaccharide raw materials are glucose and xylose (Oldham et al., 2013). For some time, sugar-based surfactants have been prepared by glycochemical methods with glucose (anhydrous or monohydrate), dextrose, and starch as the starting materials (El-Sukkary, Syed, Aiad, & El-Azab, 2008; Rather & Mishra, 2013; Turner, Svensson, Adlercreutz, & Karlsson, 2007; von Rybinski & Hill, 1998; Weuthen, Kawa, Hill, & Ansmann, 1995).

Xylose is the second most abundant sugar in the cell walls of angiosperms and can be readily obtained from raw corn stover and other agricultural wastes (Chatron-Colliet et al., 2017; Chen, Shen, Kuang, & Ji, 2016; Hong et al., 2016; Liew, Salim, Zahid, & Hashim, 2015; Qian et al., 2016; Yuan, Teng, Zhong, & Ye, 2015). Accordingly, APG based on xylose or xylan instead of glucose, maltose, and starch as raw material will be a potential hot research topic. Indeed, enzymatic/microbial, Koenigs–Knorr reaction or Fischer glycosylation reactions can be used to synthesis xylose-based surfactants that could be a useful class of xylose derivatives (Bouxin, Marinkovic, Bras, & Estrine, 2010; Chatron-Colliet et al., 2017; Damez et al., 2007; Das et al., 2017; Ochs, Muzard, Plantier-Royon, Estrine, & Rémond, 2011; Satgé, Bras, Hémin, & Muzart, 2005). Surface activity has been reported such as the surface tension of octyl β-D-xyloside and octyl α/β-D-xyloside was 30 and 27 mN m<sup>-1</sup>, at their critical micelle concentration (CMC) ( $5.72 \times 10^{-2}$  and  $3.63 \times 10^{-3}$  mol L<sup>-1</sup>), respectively (Kuang et al., 2016; Liew et al., 2015).

It is generally known that both of the hydrophilic–lipophilic balance (HLB) number and the water solubility of any sugar-based surfactant alkyl glycoside should

decrease gradually with the increase of its alkyl chain for same hydrophilic glycosyl head (Kuang et al., 2016). The water solubility is high when the HLB number is large. However, if the alkyl chain is too short (hydrophilic group is relatively large), the ideal directional arrangement on the surface of the solvent is affected leading to low surface activity (Kuang et al., 2016). If the alkyl chain is too long, the corresponding HLB number is rather small, there is weak water solubility and it is not easy to form micelles in water and reduce the surface tension.

Meanwhile, the water solubility of any sugar-based surfactants also decreases gradually with the decrease in the volume of the glycosyl head group for same alkyl chain length. As shown in Fig. 1, alkyl glycoside changes from alkyl glucoside, alkyl galactoside, and alkyl maltoside with bigger hydrophilic head to alkyl xyloside with smaller hydrophilic head. Despite the low toxicity toward human cells and good performance in diverse applications, alkyl xyloside has the weakest water solubility as it lacks a hydrophilic hydroxymethyl group (Bálint, J., Egri, G., Kolbert, A., Dianóczy, C., Fogassy, E., Novák, L., & Poppe, L., 1999; Renciu, D., Blacque, O., Vorlickova, M., & Spingler, B., 2013; Tardy-Planechaud, S., Fujimoto, J., Lin, S. S., & Sowers, L. C., 1997) on the C5 carbon. This difficult technical issue should be considered carefully in order to take full advantage of the cheap, economic, and renewable resource material xylose (Bayach et al., 2016).

In order to improve the water solubility of alkyl β-D-xylopyranoside, based on the research of predecessors (Bayach et al., 2016; Chen, Li, et al., 2016), we introduced an oxyethylene fragment (–OCH<sub>2</sub>CH<sub>2</sub>–) as a hydrophilic spacer to design an array of novel alkoxyethyl β-D-xylopyranosides (**6**) as shown in Fig. 2. The alkoxyethyl β-D-xylopyranosides were prepared by the trichloroacetimidate method (Fig. 3), and their physicochemical properties including water solubility, emulsifying property, foaming property, surface tension, thermotropic liquid crystalline (LC) property, and moisture-absorption property were investigated. By systematically varying the length of the hydrophobic tail, water solubility and structure–property relationships were investigated. Compared with the same alkyl-chain-length alkyl xylopyranoside (Kuang et al., 2016), the new designed alkoxyethyl β-D-xylopyranoside should be a value-added sugar-based nonionic surfactant since longer alkyl chain

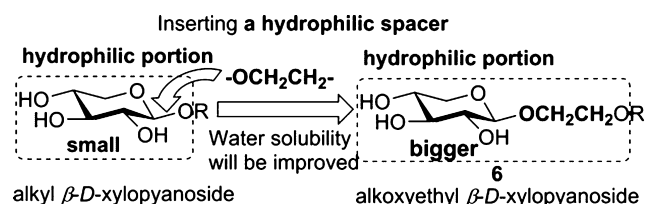


**Fig. 2** A hydrophilic spacer is inserted into alkyl β-D-xylopyranoside

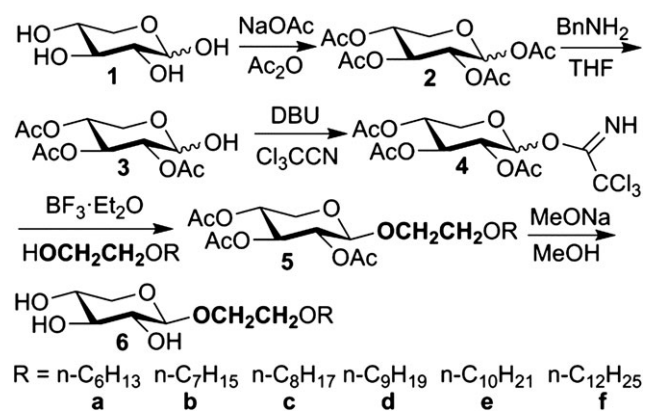


Fig. 3 Synthesis of alkoxyethyl β-D-xylopyranoside

length can be employed to achieve appropriate water solubility and surface activity for the xylopyranoside due to the introduction of the hydrophilic oxyethene spacer.

## Experimental Section

### Instrumental Analysis

The chemical structures of the synthesized alkoxyethyl β-D-xylopyranoside were confirmed using <sup>1</sup>H NMR spectroscopy using a Bruker Avance 400 spectrometer (Bruker Daltonics Inc., Fällanden, Switzerland) for solutions in CDCl<sub>3</sub>, D<sub>2</sub>O, or DMSO-*d*<sub>6</sub>. Molecular mass (MS) was measured using a Bruker Autoflex III smartbean MALDI-TOF spectrometer (Bruker Daltonics Inc., Bremen, Germany). High-resolution mass spectrum (HRMS) was measured using a Thermo Scientific LTQ Orbitrap XL (Thermo Fisher Scientific, 168 Third Avenue Waltham, USA). Melting point (mp) was obtained with an X-4 digital mp apparatus. Liquid crystal properties were observed with a DM-LM-P polarization microscope (Leica, Ernst-Leitz-Strasse 17-37 Wetzlar, 35578, Germany). Crystallinity was assessed by differential scanning calorimetry (DSC) on a TA Q10 instrument (TA Instruments, 159 Lukens Drive, New Castle, USA) under a nitrogen atmosphere at a heating or cooling rate of 5 °C min<sup>-1</sup> over 0–100 °C temperature range. Surface tension was measured by the maximum bubble pressure method (MBPM) using a DP-A precision digital pressure gauge (Nanjing Sangli electronic equipment factory, Nanjing, China). Thin-layer chromatography (TLC) was carried out on preactivated silica gel HF<sub>254</sub> by charring detection with a H<sub>2</sub>SO<sub>4</sub>/MeOH solution.

### Synthesis

All raw materials were chemical or analytical grade. As shown in Fig. 3, with D-xylose (**1**) as raw material, 2,3,4-tri-*O*-acetyl-β-D-xylopyranosyl trichloroacetimidate (**4**) was

readily prepared by three reaction steps including acetylation, selective deprotection of protecting groups at the C-1 position, and reaction with trichloroacetoneitrile. The donor **4** was coupled with a monoalkyl ethers of ethylene glycol to afford selectively 1,2-*trans* alkoxyethyl 2,3,4-tri-*O*-acetyl-β-D-xylopyranoside (**5**). The intermediate was then deacetylated to obtain the target product alkoxyethyl β-D-xylopyranoside (**6**). The detailed synthetic procedure was compiled in Appendix S1 (Supporting Information).

### HLB Number

The HLB of alkoxyethyl β-D-xylopyranosides (**6a–6f**) was calculated from Eq. 1 using Griffin's method (Abeyrathne, Perera, & Karunaratne, 2013).

$$\text{HLB} = \frac{20X}{X+A} \quad (1)$$

where *X* and *A* are the MS of the hydrophilic and lipophilic portion of the β-D-xylopyranoside (**6a–6f**), respectively.

### Solubility Properties

The solubility of xylopyranoside (**6a–6f**) was measured in different solvents (water, ethanol, and ethyl acetate) at room temperature (25 °C) according to the literature (Chen, Li, Chen, Ji, & Shen, 2017; Li, 2007). The xylopyranoside (**6a–6f**) was weighed in the test cup and a certain amount of solvent was accurately introduced into the same cup and placed on the bed and waved for 1 h. Extra solvent was carefully added dropwise until the substance completely dissolved. The solubility can be calculated according to the total consumption of the solvent.

### Dissolution Enthalpy and Entropy

According to the literature (Chen, Li, et al., 2016), the water solubility of the xylopyranoside (**6a–6e**) was measured as a function of temperature (25, 30, 35, 40, and 45 °C), and Eq. 2 was used to fit the solubility (*x<sub>A</sub>*):

$$\ln x_A = A + \frac{B}{T} \quad (2)$$

where the *A* and *B* values were achieved with least squares fitting of the experimental data and the *T* represented the temperature in Kelvin. Equations 3 and 4 were obtained based on Gibbs–Duhem equation (Kuang et al., 2016).

$$\Delta_{\text{sol}}H = RT^2 \left( \frac{d \ln x_A}{dT} \right)_P \quad (3)$$

$$\Delta_{\text{sol}}S = RT \left( \frac{d \ln x_A}{dT} \right)_P \quad (4)$$

Equations 5 and 6 were deduced to obtain the dissolution enthalpy and entropy from Eqs. 2–4.

$$\Delta_{\text{sol}}H = -RB \quad (5)$$

$$\Delta_{\text{sol}}S = -\frac{RB}{T} \quad (6)$$

### Emulsification Properties

According to the literature (Han, Yang, Liu, Wang, & Gao, 2015), a 20.0 mL aqueous solution of alkoxyethyl  $\beta$ -D-xylopyranoside (**6a–6e**) (0.25%) and 20.0 mL toluene were accurately added into a 100-mL measuring cylinder with stopper at 25 °C. The cylinder was covered and shaken; the mixture was then allowed to stand for 1.0 h; and the volume of the water layer, the emulsion layer, and the oil layer were recorded, respectively. Similarly, the emulsification of alkoxyethyl  $\beta$ -D-xylopyranoside in rapeseed oil/water system was also tested; the corresponding volumes of the water layer, the emulsion layer, and the oil layer were also recorded, respectively.

### Foaming Properties

According to the literature (Chen, Li, et al., 2016; Gao, Yang, Bai, & Zhang, 2014), a 100 mL aqueous solution of the alkoxyethyl  $\beta$ -D-xylopyranoside (**6a–6d**) (0.25%) was prepared at 25 °C, and 10 mL of the solution was taken into a 100 mL measuring cylinder with stopper. The measuring cylinder was covered and shaken vigorously up and down for 1 min and the volume of foam at the moment ( $H_0$ ) was recorded. After the mixed solution was kept static state for 5 min, the volume of foam ( $H_5$ ) was recorded. According to Eq. 7, the rate ( $\nu$ ) of bubble disappearance was calculated, which was used to estimate the foaming stability.

$$\nu = \frac{V_0 - V_5}{t} \left( \frac{\text{cm}^3}{\text{s}} \right) \quad (7)$$

### Interfacial Properties

According to the MBPM (Chen, Li, et al., 2016; Eastoe & Dalton, 2000; Fainerman, Kazakov, Lylyk, Makievski, & Miller, 2004), a series of different concentrations of aqueous solution of xylopyranoside (**6a–6d**) were prepared at 25 °C to record the corresponding maximum additional stress ( $\Delta p$ ); with secondary distilled water as a reference, the surface tension ( $\gamma$ ) of different concentrations was further calculated according to the Laplace formula (Eq. 8). The surface tension ( $\gamma$ ) and the concentration ( $C$ ) were drawn out from all the obtained data. According to Eqs. 9

and 10, the saturated adsorption amount ( $\Gamma_{\text{max}}$ ) and the average molecular area ( $A_{\text{min}}$ ) were achieved, respectively.

$$\gamma = k\Delta p \quad (8)$$

$$\Gamma_{\text{max}} = -\frac{1}{nRT} \cdot \left( \frac{d\gamma}{d\ln C} \right) \quad (9)$$

$$A_{\text{min}} = \frac{1}{N_A \Gamma_{\text{max}}} \quad (10)$$

Since xylopyranoside (**6a–6d**) is classified as a nonionic surfactant,  $n = 1$ ;  $R = 8.314 \text{ KJ mol}^{-1} \text{ K}^{-1}$ ;  $T$  stands for thermodynamic temperature (K);  $d\gamma/d\ln C$  represented the slope of the fitted curve before the inflection point and  $N_A$  is Avogadro constant. The effectiveness ( $\pi_{\text{CMC}}$ ) was obtained from Eq. 11.

$$\pi_{\text{CMC}} = \gamma_0 - \gamma_{\text{CMC}} \quad (11)$$

In Eq. 11,  $\gamma_0$  is the surface tension of distilled water and  $\gamma_{\text{CMC}}$  was the surface tension at the CMC. The efficiency and the ability to reduce surface tension ( $pC_{20}$ ) were calculated by Eq. 12.

$$pC_{20} = -\log C_{20} \quad (12)$$

In Eq. 12,  $C_{20}$  is the concentration when the solution surface tension was ( $\gamma_0$ ) 20 mN m<sup>-1</sup>.

The standard micellization and adsorption free energies ( $\Delta G_{\text{mic}}$  and  $\Delta G_{\text{ads}}$ ) of alkoxyethyl  $\beta$ -D-xylopyranoside were calculated from Eqs. 13 and 14, respectively.

$$\Delta G_{\text{mic}} = RT \ln(\text{CMC}) \quad (13)$$

$$\Delta G_{\text{ads}} = \Delta G_{\text{mic}} - \frac{\pi_{\text{CMC}}}{\Gamma_{\text{max}}} \quad (14)$$

### Thermotropic Phase Behavior

According to the known literature (Hashim et al., 2011; Liew et al., 2015), the thermotropic phase behavior of alkoxyethyl  $\beta$ -D-xylopyranoside (**6a–6f**) was evaluated by polarized microscopy (POM) with a heating rate of 3 °C min<sup>-1</sup>. Both the mp and clearing point (Cp) were recorded. Crystallinity was assessed by DSC method on a TA Q10 instrument under a nitrogen atmosphere at a heating and cooling rate of 5 °C min<sup>-1</sup> over the temperature range of 0–100 °C.

### Hygroscopicity

According to the literature method (Ying, Yang, Yi, & Xu, 2007), the hygroscopicity of alkoxyethyl  $\beta$ -D-xylopyranoside



**Table 1** HLB number of alkoxyethyl  $\beta$ -D-xylopyranoside

Glycoside	6a	6b	6c	6d	6e	6f
HLB number	13.9	13.2	12.6	12.1	11.6	10.7

(**6a–6f**) was determined by the weighing method. The dried xylosides were accurately weighted (1.00 g) and placed into bottles of the same size, the bottles with the samples was placed into a desiccator, and kept with the constant temperature and constant relative humidity (RH) for a period of time. The additional weight gain was measured to estimate the hygroscopic ability from its surroundings by Eq. 15.

$$W\% = \frac{W_t - W_0}{W_0} \times 100\% \quad (15)$$

In Eq. 15,  $W_0$  is the weight of dried sample before testing, and  $W_t$  is the weight of sample after testing for  $t$  hours.

## Results and Discussion

### Preparation and Structure Characterization

Alkoxyethyl  $\beta$ -D-xylopyranosides (**6a–6f**,  $n = 6–12$ ) may be obtained by a glycosidase enzyme that is able to catalyze the formation of glycosides in a green and highly selective process, but the operating conditions such as water activity, temperature, time of incubation, pH value, nature of the substrate, resource, and activity of enzyme will affect their process, yield, and cost. Nevertheless, the technique is mainly in the experimental stage (Chatron-Colliet et al., 2017; Ochs et al., 2011).

Fischer glycosylation reaction does not afford 1,2-trans alkoxyethyl  $\beta$ -D-xylopyranoside, but an inseparable mixture of  $\alpha/\beta$  anomers (Bouxin et al., 2010; Damez et al., 2007). Koenigs–Knorr method can achieve 1,2-trans  $\beta$ -D-xylopyranoside, but there are some disadvantages such as high-cost catalyst, environmentally unfriendly, unsuitable for industrial production (Geetha & Tyagi, 2012; Satgé et al., 2005; Xu et al., 2012). In spite of this, the Schmidt method was selected to prepare a series of 1,2-trans alkoxyethyl  $\beta$ -D-xylopyranosides (**6a–6f**,  $n = 6–12$ ) by the neighboring group participation as shown in Fig. 3. The detailed synthetic procedure is described in Appendix S1. The characterization data of alkoxyethyl 2,3,4-tri-*O*-acetyl- $\beta$ -D-xylopyranosides (**5a**,  $n = 6$ ) and alkoxyethyl  $\beta$ -D-xylopyranosides (**6a–6f**,  $n = 6–12$ ) are also shown in Appendix S1.

For some glycosides including xylopyranoside, glucopyranoside, 2-acetamido-2-deoxy- $\beta$ -glucopyranoside, and galactopyranoside, their anomers can be handily confirmed from their coupling constant  $J_{1,2}$  of H-1 at  $^1\text{H}$  NMR spectrum. For a coupling compound hexyloxyethyl 2,3,4-tri-*O*-acetyl- $\beta$ -D-xylopyranoside (**5a**), its chemical shift ( $\delta$ ) (ppm)

and coupling constant ( $J_{1,2}$ ) of H-1 were  $\delta$  4.57 (d,  $J = 6.8$  Hz) to affirm a 1,2-trans structure. For deprotected target compounds alkoxyethyl  $\beta$ -D-xylopyranosides (**6a–6f**), their chemical shifts ( $\delta$ ) (ppm) and coupling constants ( $J_{1,2}$ ) of H-1 for the xylopyranosides (**6a–6f**) were  $\delta$  4.41 (d,  $J = 7.8$  Hz) (**6a**), 4.33 (d,  $J = 7.8$  Hz) (**6b**), and 4.40 (d,  $J = 7.4$  Hz) (**6c**) with  $\text{D}_2\text{O}$  as the solvent,  $\delta$  4.11 (d,  $J = 7.6$  Hz) (**6d**), 4.11 (d,  $J = 7.6$  Hz) (**6e**) with  $\text{DMSO-}d_6$  as the solvent, 4.13 (d,  $J = 7.6$  Hz) (**6f**) with  $\text{DMSO-}d_6/\text{D}_2\text{O}$  as the solvent, all of the prepared  $\beta$ -D-xylopyranosides (**6a–6f**,  $n = 6–12$ ) were further approved to possess 1,2-trans  $\beta$ -glycosyl bond since their coupling constant  $J_{1,2}$  of H-1 is in the range of 4.0–8.0 Hz by the  $^1\text{H}$  NMR spectroscopy (Bouxin et al., 2010; Chen & Kong, 2002; Kuang et al., 2016; Xu et al., 2012).

### HLB Number and Solubility

According to Eq. 1, the calculated HLB numbers of alkoxyethyl  $\beta$ -D-xylopyranosides (**6a–6f**,  $n = 6–12$ ) are shown in Table 1. In Table 1, the HLB numbers decrease with increasing alkyl chain length. All HLB numbers are at the range of 10.7–13.9, which illustrates that all of them are hydrophilicity since  $\text{HLB} > 10$ . By comparison, three alkyl polyglucosides (APG) had HLB numbers of 13 (capryl glucoside, APG- $\text{R}_{8-10}\text{DP}_{1.4}$ ), 11.9 (coco glucoside, APG- $\text{R}_{8-14}\text{DP}_{1.3}$ ), and 11.2 (lauryl glucoside, APG- $\text{R}_{12-14}\text{DP}_{1.5}$ ), respectively (Ríos et al., 2016). Therefore, our prepared alkoxyethyl  $\beta$ -D-xylopyranosides (**6a–6f**) also achieved around the APG HLB values by introducing a hydrophilic spacer ( $-\text{OCH}_2\text{CH}_2-$ ) instead of increasing DP.

The solubilities of alkoxyethyl  $\beta$ -D-xylopyranosides (**6a–6f**,  $n = 6–12$ ) in  $\text{H}_2\text{O}$ , EtOH, and AcOEt at  $25^\circ\text{C}$  are shown in Fig. 4. The solubilities in  $\text{H}_2\text{O}$ , EtOH, and AcOEt

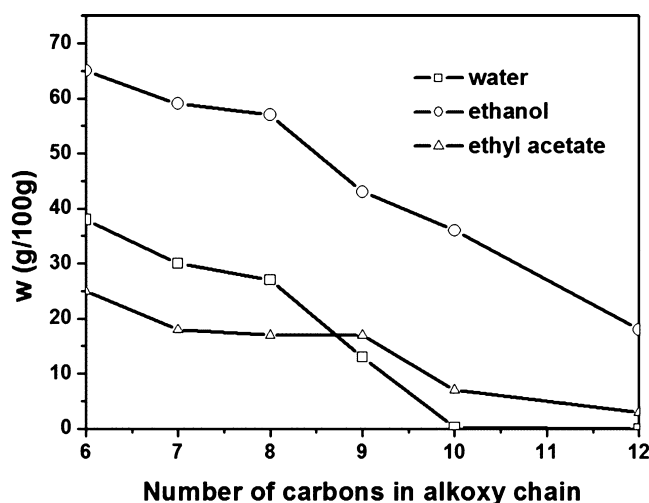


**Fig. 4** Solubility of alkoxyethyl  $\beta$ -D-xylopyranoside in different solvent

all decrease with increasing alkyl chain length. The solubility in EtOH was greater than the solubility in H<sub>2</sub>O. Dodecyloxyethyl  $\beta$ -D-xylopyranoside (**6f**) still dissolved in EtOH in spite of the carbon number ( $n$ ) of its alkyl chain reaching as high as 12; however, decyloxyethyl  $\beta$ -D-xylopyranoside (**6e**) ( $n = 10$ ) had poor solubility in H<sub>2</sub>O, only as low as 0.2 g per 100 g, and **6f** ( $n = 12$ ) did not dissolve in H<sub>2</sub>O. Other alkoxyethyl  $\beta$ -D-xylopyranosides (**6a–6d**) ( $n = 6–9$ ) were observed to have excellent solubility in H<sub>2</sub>O, EtOH, and AcOEt, and their calculated HLB numbers were all larger than 12.0.

In the literature (Chen, Li, et al., 2016; Kuang et al., 2016), with the six-membered C5O ring, there is a proton instead of the strong hydrophilic hydroxymethyl group at the C5 position on the xylosyl headgroup; hence, the water solubility of alkyl  $\beta$ -D-xylopyranoside decreased gradually with the increase of alkyl chain as it has a smaller head-group volume that naturally renders its less hydrophilic compared to other glycoside such as alkyl  $\beta$ -D-glucopyranoside and alkyl  $\beta$ -D-maltoside. Hexyl  $\beta$ -D-xylopyranoside ( $n = 6$ ) has poor solubility in water. To our delight, the oxyethylene fragment ( $-\text{OCH}_2\text{CH}_2-$ ) as a hydrophilic spacer was introduced to obtain a series of xylopyranosides, i.e., alkoxyethyl  $\beta$ -D-xylopyranosides (**6a–6f**), and they have novelty and better solubility in water with comparison of the same alkyl chain length of alkyl  $\beta$ -D-xylopyranosides. There are totally similar improving trends of the solubilities in ethanol for comparing alkoxyethyl  $\beta$ -D-xylopyranosides (**6a–6f**) and alkyl  $\beta$ -D-xylopyranosides with the same alkyl chain length as well.

As disclosed in the literature (Ochs et al., 2011), partitioning of octyl oligoxyloside between aqueous and octanol phase depends on the average degree of polymerization (DP), octyl  $\beta$ -D-xyloside (95%), octyl  $\beta$ -D-xylobioside (88%), and octyl  $\beta$ -D-xylotrioside (62%) were mainly localized in the octanol phase. The result could be considered as octyl  $\beta$ -D-xylopyranoside (HLB = 11.4 < 12.0) had very small water solubility (0.05 g per 100 g [water]) (Kuang et al., 2016), octyl  $\beta$ -D-xylobioside (HLB = 14.3) and octyl  $\beta$ -D-xylotrioside (HLB = 15.7) should have higher water solubility though the data were not found in literature, but the two anomeric pure alkyl oligoxylosides are more difficult to prepare than alkoxyethyl  $\beta$ -D-xyloside with glycochemistry. For the alkyl polyxylosides, Krafft point was also used to evaluate the water solubility, the Krafft points of octyl polyxyloside (DP = 1.2), decyl polyxyloside (DP = 1.1), and dodecyl polyxyloside (DP = 1.2) were 21, 36.2, and 44.9 °C, respectively, indicating that octyl polyxyloside (DP = 1.2, HLB = 12.2) had rather low water solubility, decyl polyxyloside (DP = 1.1, HLB = 10.7), and dodecyl polyxyloside (DP = 1.2, HLB = 10.2) have low water solubility as they have low DP (near 1) (Renault, Portella, Marinkovic, & Estrine, 2012). For alkyl glucoside

and alkyl galactoside, e.g., octyl  $\beta$ -D-glucoside, octyl  $\alpha$ -D-glucoside, octyl  $\beta$ -D-galactoside, and octyl  $\alpha$ -D-galactoside have same HLB number (12.3), and their water solubilities were 0.60 (Liu et al., 2013), 0.05 (Li, Chen, Chen, Shen, & Ji, 2016), 1.07, and 10.02 g/100 mL (water) at room temperature (Chen et al., 2017; Chen, Li, et al., 2016). They are different from each other, indicating that the glycosyl head and anomeric configuration affect the water solubility in spite of identical HLB numbers. APG with DP from 1 to 5 containing alkyl chains from 6 to 14 carbons are soluble in water, such as C8/C10 polyglucosides, C9–11 polyglucosides, and C12/C14 polyglucosides, they are considered as water solubility; but these molecules with 16–22 carbon atoms are oil-soluble. Their water solubility increases with increasing DP (Sulek, Ogorzałek, Wasilewski, & Klimaszewska, 2013). Of course, cloud point can also be used to evaluate water solubility to some extent (von Rybinski & Hill, 1998).

As foundational research, alkyl glycoside such as alkyl  $\beta$ -D-xylopyranoside or its derivative alkoxyethyl  $\beta$ -D-xylopyranoside and other pure compounds are easy to obtain exact data on water solubility, but mixtures of alkyl (poly) glycosides, such as APG, alkyl  $\alpha/\beta$ -glycoside, or alkyl furanose/pyranoside, are difficult to achieve exact data for water solubility.

### Dissolution Enthalpy and Entropy

The heat of solution can be defined as the change in enthalpy when a given solute is dissolved in a solvent to form a solution at a certain temperature and pressure. Moreover, the dissolution enthalpy of the solution can reflect the influence of temperature on the solute's solubility. The dissolution behavior is an endothermic process while the dissolution enthalpy has a positive value and *vice versa*.

In order to determine the dissolution enthalpy ( $\Delta_{\text{sol}}H$ ) and dissolution entropy ( $\Delta_{\text{sol}}S$ ) of alkoxyethyl  $\beta$ -D-xylopyranoside, we selected some alkoxyethyl  $\beta$ -D-xylopyranosides (**6a–6e**,  $n = 6–10$ ) that were soluble in water at room temperature as described previously, and measured their solubility at 25, 30, 35, 40, and 45 °C. The relationship between solubility ( $\ln x_A$ ) and temperature ( $1/T$ ) is shown in Fig. 5. In Fig. 5, the solubility ( $\ln x_A$ ) increased obviously as the temperature increased gradually. Moreover, for hexyloxyethyl, heptyloxyethyl, and octyloxyethyl  $\beta$ -D-xylopyranoside (**6a–6b**,  $n = 6–8$ ), the variation magnitudes of their solubilities ( $\ln x_A$ ) were smaller with increasing temperature; for decyloxyethyl  $\beta$ -D-xylopyranoside (**6e**,  $n = 10$ ), its variation was obviously larger with increase in temperature as there is a relatively steep straight line, far away from other lines of  $\beta$ -D-xylopyranosides (**6a–6d**). The values of A and B were obtained from the straight line in Fig. 1 and Eq. 2 are given in Table 2. According to Eq. 5, the values

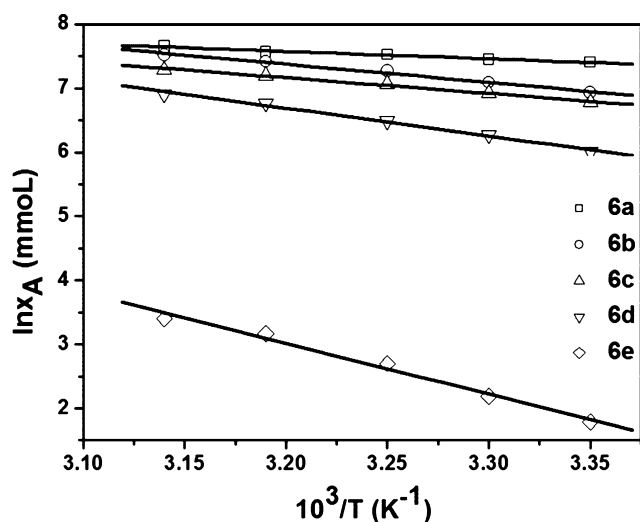


**Fig. 5** Solubility of alkoxyethyl xylopyranoside in water at different temperature

of dissolution enthalpy ( $\Delta_{\text{sol}}H$ ) of  $\beta$ -D-xylopyranosides (**6a–6e**) were calculated and given in Table 2 and  $\Delta_{\text{sol}}H > 0$ , which indicated that the dissolution process of  $\beta$ -D-xylopyranosides (**6a–6e**) is an endothermic process and that  $\Delta_{\text{sol}}H$  increases with increasing alkyl chain length.

In addition, the value of dissolution entropy ( $\Delta_{\text{sol}}S$ ) was calculated by Eq. 6. The relationship between temperature and dissolution entropy is shown in Fig. 6, and the dissolution entropy of  $\beta$ -D-xylopyranoside (**6a–6e**) decreased gradually with increasing temperature. The value of dissolution entropy of hexyloxyethyl  $\beta$ -D-xylopyranoside (**6a**) was the smallest, and that of decyloxyethyl  $\beta$ -D-xylopyranoside (**6e**) was maximal and far away other  $\beta$ -D-xylopyranosides (**6a**, **6b**), and  $\Delta_{\text{sol}}S > 0$ . In the literature (Kuang et al., 2016), both  $\Delta_{\text{sol}}H$  and  $\Delta_{\text{sol}}S$  values of alkyl  $\beta$ -D-xylopyranosides ( $n = 4–9$ ) also decreased with increasing temperature. The  $\Delta_{\text{sol}}S$  values increased with the increase of alkyl chain. The oxyethene fragment ( $-\text{OCH}_2\text{CH}_2-$ ) as a hydrophilic spacer was introduced to obtain novel alkoxyethyl  $\beta$ -D-xylopyranoside, with increased HLB number and improved water solubility, but did not change the trend in the dissolution process. Hence, both should have the same endothermic and entropic driving force because both of  $\Delta_{\text{sol}}H > 0$  and  $\Delta_{\text{sol}}S > 0$  during the dissolution process of alkyl  $\beta$ -D-xylopyranosides ( $n = 4–9$ ) and alkoxyethyl  $\beta$ -D-xylopyranosides (**6a–6e**,  $n = 6–10$ ) in water.

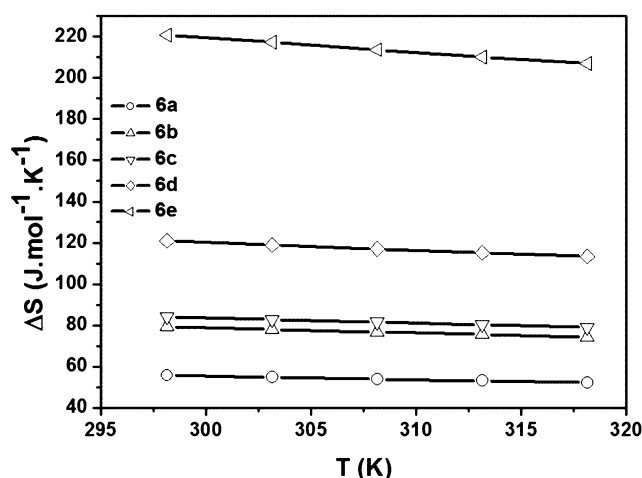


**Fig. 6** Dissolution entropy of xylopyranosides at different temperature

### Foaming Properties

APG generally have rich and delicate foam. In this study, the foaming property of alkoxyethyl  $\beta$ -D-xylopyranosides (**6a–6d**,  $n = 6–9$ ) including foaming characteristics and foam stability was investigated. In Fig. 7, the foaming ability, i.e., initial volume ( $H_0$ ), of alkoxyethyl  $\beta$ -D-xylopyranosides (**6a–6d**) first increased and then decreased with increasing alkyl chain length, final volume ( $H_5$ ) also changed in the same manner; however, rate ( $\nu$ ) of bubble disappearance shows slight differences. In addition, octyloxyethyl  $\beta$ -D-xylopyranoside (**6c**,  $n = 8$ ) and nonyloxyethyl  $\beta$ -D-xylopyranoside (**6d**,  $n = 9$ ) had excellent foaming ability, and octyloxyethyl  $\beta$ -D-xylopyranoside (**6c**,  $n = 8$ ) has the strongest foaming ability, and its  $H_5$  was as high as 35 mL, but the nonyloxyethyl  $\beta$ -D-xylopyranoside (**6d**) had best foam stability as its  $\nu$  was as low as  $0.01 \text{ mL s}^{-1}$ .

### Emulsification Properties

The emulsification of alkoxyethyl  $\beta$ -D-xylopyranoside (**6a–6e**,  $n = 6–10$ ) in rapeseed oil/water system and in toluene/water system was investigated. In Figs. 8 and 9, the volume of the oil-in-water (O/W) emulsion layer first increased and then decreased in the same way in both systems with increasing alkyl chain length. In both systems, emulsifying ability of nonyloxyethyl  $\beta$ -D-xylopyranoside (**6d**,  $n = 9$ )

**Table 2** Parameter of Eq. 2 and dissolution enthalpy for different solution

Glycoside	<b>6a</b>	<b>6b</b>	<b>6c</b>	<b>6d</b>	<b>6e</b>
A	13.96	16.48	16.91	20.57	28.36
B	−1999.29	−2844.24	−3022.05	−4338.55	−7919.63
$\Delta_{\text{sol}}H$ (kJ mol <sup>−1</sup> )	16.62	23.65	25.13	36.07	65.85

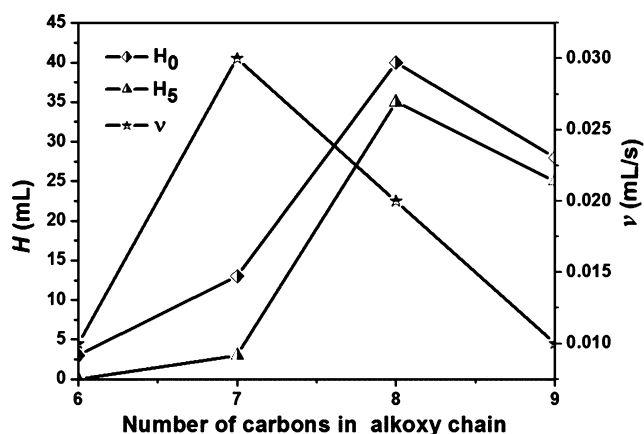


Fig. 7 Foaming ability of alkoxyethyl  $\beta$ -D-xylopyranoside (**6a–6d**)

was the strongest, the emulsified layer had as high as 30 mL in rapeseed oil/water system and 40 mL in toluene/water system, respectively. In spite of its weak water solubility, the possible reasons may be that the nonyl group was the most excellent by its weak hydrophobic bonds and fine flexible chain in making the strongest emulsifying ability as its calculated HLB was 12.1.

For the rapeseed oil/water system, hexyloxyethyl xylopyranoside (**6a**,  $n = 6$ ) had poor emulsifying ability; heptyloxyethyl and octyloxyethyl xylopyranoside (**6b**, **6c**,  $n = 7, 8$ ) had only weak emulsifying ability; and formed Winsor type III systems (water layer, emulsifying layer and oil layer), nonyloxyethyl, and decyloxyethyl xylopyranosides (**6d**, **6e**,  $n = 9, 10$ ) shows the formation of Winsor II systems (Ruckenstein, 1996). Moreover, for the toluene/water system, both of hexyloxyethyl and heptyloxyethyl xylopyranosides (**6a**, **6b**,  $n = 6, 7$ ) show weak O/W emulsifying ability, and three xylopyranosides (**6a–6c**,  $n = 6–8$ ) participated in the formation of the Winsor type III systems,

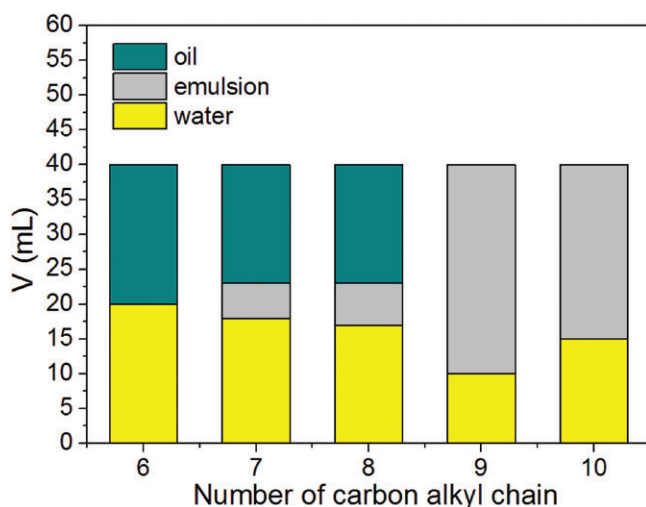


Fig. 8 Emulsifying ability of xylopyranoside (**6a–6e**) in rapeseed oil/water system

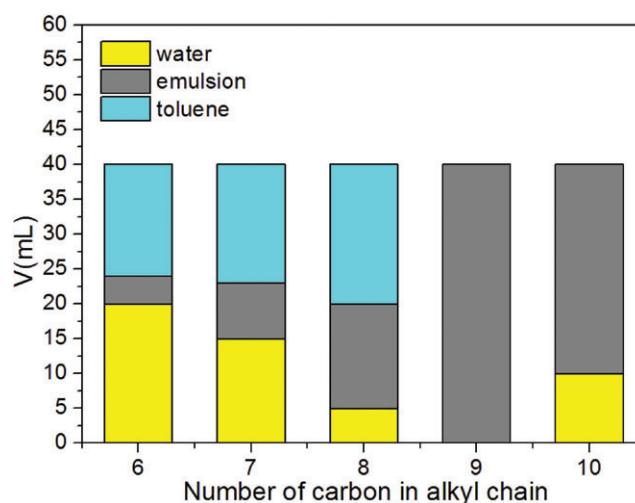


Fig. 9 Emulsifying ability of xylopyranoside (**6a–6e**) in toluene/water system

nonyloxyethyl xylopyranoside (**6d**,  $n = 9$ ) had the strongest emulsifying ability and participated in the formation of single layer, i.e., an emulsifying layer, decyloxyethyl xylopyranoside (**6e**,  $n = 10$ ) participated in the formation of a Winsor type II system. The xylopyranoside (**6a–6e**) were observed to have slightly stronger emulsifying ability in toluene/water system than that in rapeseed oil/water system because there were higher emulsion layer volumes in toluene/water system than in rapeseed oil/water system.

### Interfacial Properties

The relationship between the concentration of alkoxyethyl  $\beta$ -D-xylopyranosides (**6a–6d**,  $n = 6–9$ ) and the surface tension in their aqueous solution was investigated at 25 °C and the results are shown in Fig. 10 and Table 3. In Fig. 10,

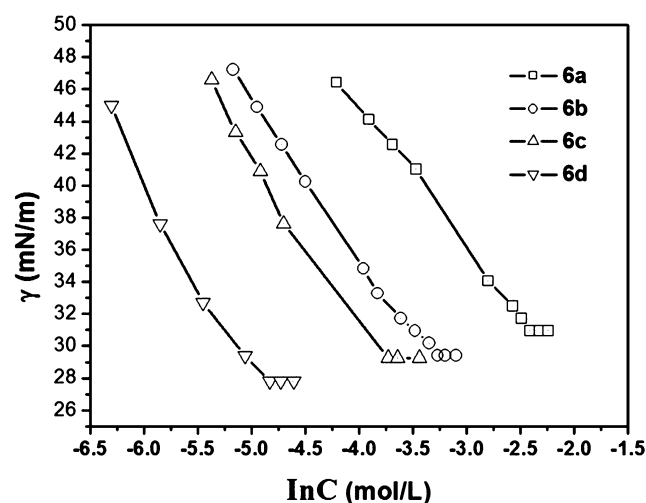


Fig. 10 Relationship between surface tension and concentration of xylopyranoside



**Table 3** Adsorption parameter of  $\beta$ -D-xylopyranoside at 25 °C

Glycoside	<b>6a</b>	<b>6b</b>	<b>6c</b>	<b>6d</b>
CMC (mol L <sup>-1</sup> )	$9.00 \times 10^{-2}$	$3.81 \times 10^{-2}$	$2.42 \times 10^{-2}$	$7.96 \times 10^{-2}$
$\gamma_{\text{CMC}}$ (mN m <sup>-1</sup> )	30.96	29.41	29.26	27.80
$d\gamma/d\ln C$	-8.79	-9.45	-10.36	-11.59
$\Gamma_{\text{max}}$ (10 <sup>-6</sup> mol m <sup>-2</sup> )	3.55	3.81	4.18	4.68
$A_{\text{mn}}$ (Å <sup>2</sup> )	46.79	43.60	39.74	35.50
$\pi_{\text{CMC}}$ (mN m <sup>-1</sup> )	41.01	42.56	42.71	44.17
pC <sub>20</sub>	2.08	2.48	2.59	3.04
$\Delta G_{\text{mic}}$ (kJ m <sup>-1</sup> )	-5.97	-8.10	-9.23	-11.98
$\Delta G_{\text{ads}}$ (kJ m <sup>-1</sup> )	-17.52	-19.27	-19.45	-21.42

there is an inflection point for each curve and the concentration at the inflection point is considered as the CMC. The surface tension ( $\gamma$ ) of the aqueous solution of the  $\beta$ -D-xylopyranoside (**6a–6d**) gradually decreased with increasing concentration and reached a specific low value ( $\gamma_{\text{CMC}}$ ) at the CMC. The surface tension of the aqueous solution of nonyloxyethyl  $\beta$ -D-xylopyranoside (**6d**,  $n = 9$ ) was as low as 27.80 mN m<sup>-1</sup> at its CMC. Different alkoxyethyl  $\beta$ -D-xylopyranoside had different CMC value and the value depends on the length of alkyl chain, the longer the alkyl chain, the lower the CMC value, which indicated that there was higher surface activity for alkoxyethyl  $\beta$ -D-xylopyranoside with longer chain in the range of  $n = 6–9$ . In Table 3, the average molecular area ( $A_{\text{min}}$ ) of alkoxyethyl  $\beta$ -D-xylopyranoside (**6a–6d**,  $n = 6–9$ ) is also shown to decrease with increasing alkyl chain length.

In Table 3, the effectiveness ( $\pi_{\text{CMC}}$ ) increased for  $\beta$ -D-xylopyranoside (**6a–6d**) with increasing alkyl chain length, the higher the effectiveness of surface tension reduction at the CMC, the stronger the surface activity. As shown in Table 3, the efficiency (pC<sub>20</sub>) increased also for  $\beta$ -D-xylopyranoside (**6a–6d**) with increasing alkyl chain length, the larger pC<sub>20</sub> value, the greater the tendency of the surfactant to adsorb at the air/water interface (Chen, Li, et al., 2016). Hence, nonyloxyethyl  $\beta$ -D-xylopyranoside (**6d**) had the strongest surface activity because its effectiveness ( $\pi_{\text{CMC}}$ ) and efficiency (pC<sub>20</sub>) were largest.

In addition, the micellization free energy ( $\Delta G_{\text{mic}}$ ) in the solution and the adsorption free energy ( $\Delta G_{\text{ads}}$ ) in the surface layer of alkoxyethyl  $\beta$ -D-xylopyranosides (**6a–6d**,  $n = 6–9$ ) in aqueous solution were negative as shown in Table 3, and their values became more negative with increasing alkyl chain length, indicating that the micelle and surface adsorption in solution is a spontaneous process involving the hydrophobic effect (Chen, Li, et al., 2016). The  $\Delta G_{\text{ads}}$  value is more negative than the  $\Delta G_{\text{mic}}$  value, which indicated that alkoxyethyl  $\beta$ -D-xylopyranoside (**6a–6d**) was easier to adsorb at the interface to form a monolayer rather than to form micelles in solution when the concentration is below the CMC. When the concentration is

above the CMC, the surface tension ( $\gamma$ ) of the  $\beta$ -D-xylopyranoside (**6a–6d**) solution is a constant straight line because the surface concentration remains constant and the extra  $\beta$ -D-xylopyranoside is incorporated into micelles. Therefore, the spontaneous self-assembled micellization is driven by the hydrophobic effect owing to the minimization of the Gibbs free energy.

The CMC value of octyl  $\beta$ -D-glucoside (HLB = 12.3) is  $2.5 \times 10^{-2}$  mol L<sup>-1</sup> (Chen & Kong, 2002). APG, C<sub>8</sub>APG, C<sub>9</sub>APG, C<sub>10</sub>APG, and C<sub>12</sub>APG have CMC ( $\gamma_{\text{CMC}}$ ) values of  $1.71 \times 10^{-3}$  (29),  $1.23 \times 10^{-3}$  (33),  $7.81 \times 10^{-4}$  (31), and  $2.97 \times 10^{-4}$  mol L<sup>-1</sup> (32 mN m<sup>-1</sup>) (El-Sukkary et al., 2008). Two representative commercial APG had CMC values of 1.01 (capryl glucoside, APG-R<sub>8–10</sub>DP<sub>1.4</sub>, HLB = 13) and 0.15 (coco glucoside, APG-R<sub>8–14</sub>DP<sub>1.3</sub>, HLB = 11.9), respectively (Ríos et al., 2016). For the alkyl polyxylosides, the CMC ( $\gamma_{\text{CMC}}$ ) values of octyl  $\alpha/\beta$ -D-xyloside (DP = 1, HLB = 11.4) and octyl  $\beta$ -D-oligoxylosides (DP > 2) were 0.953 g L<sup>-1</sup> (i.e.,  $3.66 \times 10^{-6}$  mol L<sup>-1</sup>) (27 mN m<sup>-1</sup>) and 4.23 g L<sup>-1</sup> (27.0 mN m<sup>-1</sup>), respectively (Ochs et al., 2011). The data show that lower CMC value regardless of the alkoxyethyl  $\beta$ -D-xylopyranosides compared to other alkyl (poly)glycosides.

In the literature (Kuang et al., 2016), the surface tensions of octyl and nonyl  $\beta$ -D-xylopyranoside ( $n = 8, 9$ ) were 30.08 and 35.72 mN m<sup>-1</sup> in their aqueous solution under the CMC, respectively. And the surface tensions of octyloxyethyl and nonyloxyethyl  $\beta$ -D-xylopyranose (**6c**, **6d**,  $n = 8, 9$ ) were 29.26 and 27.80 mN m<sup>-1</sup> in their aqueous solution under the CMC in this work, respectively. Therefore, compared with the alkyl  $\beta$ -D-xylopyranoside, our synthesized alkoxyethyl  $\beta$ -D-xylopyranosides had better surface activity at the same carbon chain length.

### Thermotropic LC Properties

LC phase structures are often found in living organisms. Cellular membranes are the result of lyotropic LC phases resulting from the dissolution of phospholipids in water (de Souza et al., 2017; Lagerwall & Scalia, 2012). There

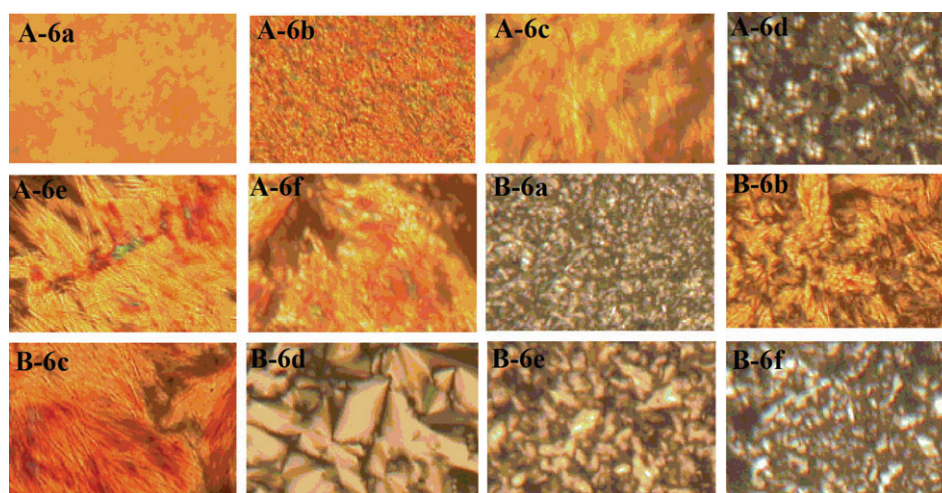


**Fig. 11** Texture of alkoxyethyl  $\beta$ -D-xylopyranoside characterized by OPM upon heating (a) and cooling (b) (magnification 200 $\times$ )

should be value in studying sugar-based amphiprotic non-ionic surfactants such as alkyl glycosides with many advantages (Hashim, Sugimura, Minamikawa, & Heidelberg, 2012) as some of them possess the LC performance. The lyotropic LC behavior and/or thermotropic LC behavior are related to its structure and other physicochemical properties, thereby the specific research results are able to provide a lot of useful information in drug delivery, gene delivery, self-organization, self-assembly and supermolecule formation, functional biomembrane, LC biological sensors, and LC-based immunodetection to some extent (Hashim et al., 2012; Lagerwall & Scalia, 2012; de Souza et al., 2017). We used a polarizing microscope (OPM) to observe the thermotropic LC behavior of the alkoxyethyl  $\beta$ -D-xylopyranosides (**6a–6f**,  $n = 6–12$ ) in the heating process to learn more about the relations between their alkyl chain length and the thermotropic LC performance, and the results are shown in Fig. 11.

In Fig. 11, the thermotropic liquid crystal texture was observed in the process of heating (A) under the polarizing microscope. Nonyloxyethyl  $\beta$ -D-xylopyranoside (**6d**,  $n = 9$ ) presented clear Maltese cross pattern texture in the process of heating, conversely, it showed fan schlieren texture in the process of cooling, the texture belonging to crystal Smetic A (Hashim et al., 2012). However, other alkoxyethyl  $\beta$ -D-xylopyranoside (**6a–6c**,  $n = 6–8$ ; **6e**,  $n = 10$ ; **6f**,  $n = 12$ ) performed indistinct, even shapeless, cross pattern

texture in the heating process, weakened obviously their fan schlieren texture to some extent and even remained obscure in cooling process.

Table 4 summarizes their mp and the Cp, both mp and Cp increase gradually with increasing alkyl chain length, and the phase transformation temperature ( $\Delta T$ ) were in the range of 9.38–15.65. Meanwhile, Fig. 12 shows the DSC thermogram of alkoxyethyl  $\beta$ -D-xylopyranoside (**6a–6f**,  $n = 6–12$ ). In Fig. 12, hexyloxyethyl  $\beta$ -D-xylopyranoside (**6a**) and heptyloxyethyl  $\beta$ -D-xylopyranoside (**6b**) show lower mp and Cp than other  $\beta$ -D-xylopyranosides (**6c–6f**,  $n = 6–12$ ) from their heat flow curves. Alkoxyethyl  $\beta$ -D-xylopyranosides (**6c–6f**,  $n = 8–12$ ) show weaker heat flow of phase transition from solid to liquid crystal; conversely, they showed stronger heat flow of phase transition from liquid crystal to isotropic liquid.

**Table 4** Phase transition temperature of alkoxyethyl  $\beta$ -D-xylopyranoside

Glycoside	<b>6a</b>	<b>6b</b>	<b>6c</b>	<b>6d</b>	<b>6e</b>	<b>6f</b>
mp ( $^{\circ}$ C)	26.38	34.79	43.12	43.48	45.29	59.24
C <sub>p</sub> ( $^{\circ}$ C)	42.03	48.25	52.50	53.82	57.55	69.46
$\Delta T$ ( $^{\circ}$ C)	15.65	13.46	9.38	10.34	12.26	10.22

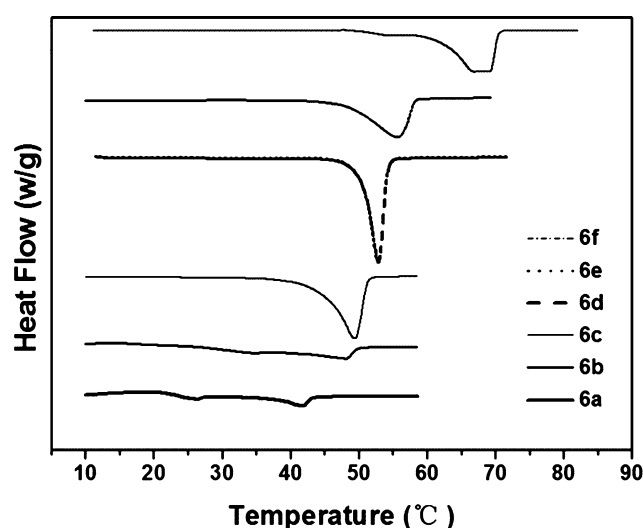


**Fig. 12** DSC curve for xylopyranoside during the heating process

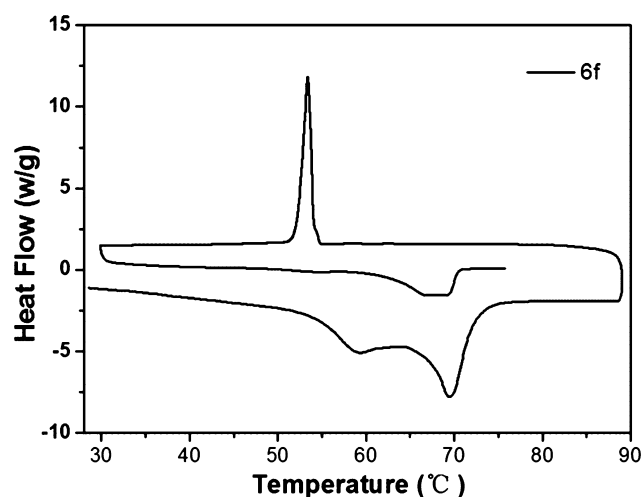


Fig. 13 DSC thermogram of dodecyloxyethyl  $\beta$ -D-xylopyranoside (**6f**)

DSC thermogram of dodecyloxyethyl  $\beta$ -D-xylopyranose (**6f**,  $n = 12$ ) is shown in Fig. 13. At first, the transition processes from crystal state to isotropic liquid state *via* liquid crystal formation upon heating at a rate of  $20\text{ }^{\circ}\text{C}$  per min. Next, an LC phase was formed on cooling at a rate of  $5\text{ }^{\circ}\text{C min}^{-1}$ . Finally, the melting peak was not observed by the second heating at a rate of  $5\text{ }^{\circ}\text{C min}^{-1}$ . The possible reason is that dodecyloxyethyl  $\beta$ -D-xylopyranose (**6f**) does not form a fine crystal state with lower symmetry under cooling from thermally induced isotropic liquid state with high symmetry by the spontaneous symmetry breaking mechanism by the change of the order parameter of Landau's phase-transition theory, and it was possible to turn into an aggregate state at the cooling; therefore, such aggregate state was observed to merge into a diffuse broad peak rather than two sharp peaks (melting peak and clearing peak).

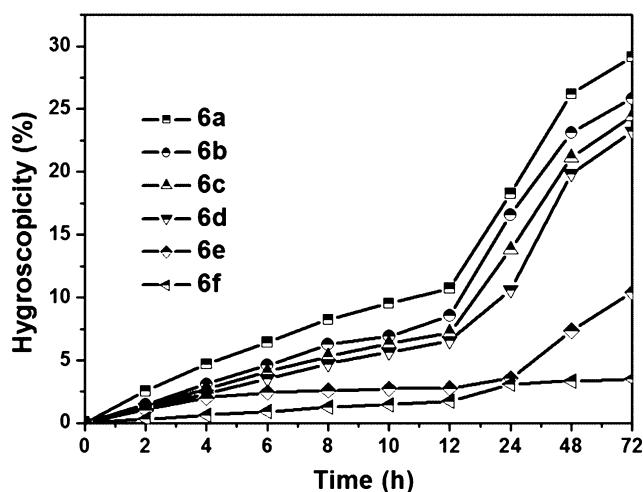


Fig. 14 Hygroscopicity of alkoxyethyl  $\beta$ -D-xylopyranoside on RH = 43%

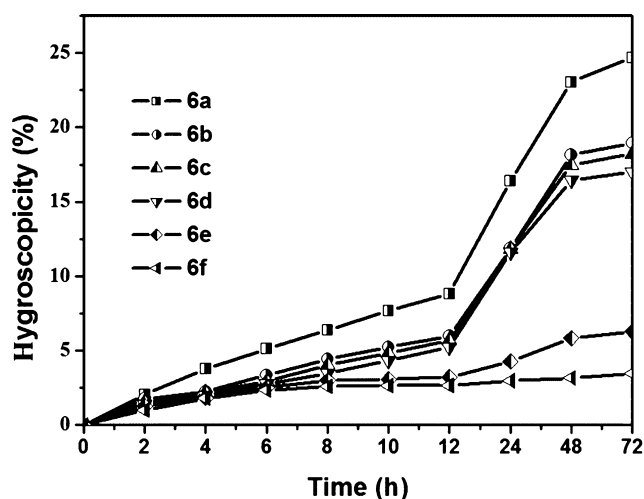


Fig. 15 Hygroscopicity of alkoxyethyl  $\beta$ -D-xylopyranoside on RH = 81%

### Hygroscopicity

Under the same humidity, the more moisture the compound absorbs, the higher the hygroscopicity. We investigated the hygroscopicity of alkoxyethyl  $\beta$ -D-xylopyranosides (**6a–6f**,  $n = 6–12$ ) according to references (Chen et al., 2017; Ying et al., 2007). The dried samples were measured under the environments of RH (RH = 43% [saturated  $\text{Na}_2\text{CO}_3$  aqueous solution] and RH = 81% [saturated  $(\text{NH}_4)_2\text{SO}_4$  aqueous solution] at  $25\text{ }^{\circ}\text{C}$ , respectively). The additional weights were recorded at the time of 2, 4, 6, 8, 10, 24, 48, and 72 h, respectively, and the results are shown in Figs. 14 (RH = 43%) and 15 (RH = 81%) according to Eq. 15.

In Figs. 14 (RH = 43%) and 15 (RH = 81%), the hygroscopicity (W%) increased with the increase of time, conversely, the hygroscopicity (W%) decreased with the increase of alkyl chain length. There was fine hygroscopicity for alkoxyethyl  $\beta$ -D-xylopyranoside (**6a–6d**,  $n = 6–9$ ) due to its shorter alkyl chain, hexyloxyethyl  $\beta$ -D-xylopyranoside (**6a**) possessed the strongest hygroscopicity (W% = 29.16% [RH 43%] and 24.68% [RH 81%]).

### Conclusion

In this study, alkyl  $\beta$ -D-xylopyranosides were upgraded to design rationally and prepare readily six alkoxyethyl  $\beta$ -D-xylopyranosides (**6a–6f**) with an oxyethene spacer by the glycochemistry method, and their 1,2-*trans* configurations were confirmed by  $^1\text{H}$  NMR spectroscopy.

An introduction of the hydrophilic space was of a benefit to the glycosides (**6a–6e**) in higher HLB number and higher water solubility than the original alkyl  $\beta$ -D-xylopyranosides with the same alkyl chain (Kuang et al., 2016);

however, dodecyloxyethyl glycoside (**6f**) did not dissolve in water because the alkyl chain is too long. By comparison, octyloxyethyl glycoside (**6c**) had the best foaming ability and better foam stability; nonyloxyethyl glycoside (**6d**) had better foaming ability, the best foam stability, and the strongest emulsifying ability. The glycosides (**6a–6d**) decreased surface tension of the aqueous solution. All glycosides (**6a–6f**) had thermotropic LC behavior, their mp and the Cp increased gradually with increasing alkyl chain, nonyloxyethyl glycoside (**6d**) showed the most distinct thermotropic liquid phase, and there was a cross pattern texture at heating and the fan schlieren texture in cooling. Their hygroscopicity (**6a–6f**) decreased with increasing alkyl chain length.

A series of anomerically pure alkoxyethyl  $\beta$ -D-xylopyranosides (**6a–6f**) were successfully obtained with a hydrophilic spacer ( $-\text{OCH}_2\text{CH}_2-$ ), and their water solubility was improved, and they had higher surface activity than the original alkyl  $\beta$ -D-xylopyranosides (Kuang et al., 2016). The foundational research should broaden their potential applications as a class of novel mild nonionic sugar-based amphiphilic surfactants with favorable ecological and toxicological properties.

**Acknowledgements** This work was supported by the National Natural Science Foundation of China (grant no. 21643010) and Hunan 2011 Collaborative Innovation Center of Chemical Engineering & Technology with Environmental Benignity and Effective Resource Utilization

## References

- Abeyrathne, A. R. N. M., Perera, A. D. L. C., & Karunaratne, D. N. (2013) Surfactant behaviour of five carbohydrate liquid crystals. *Journal of the National Science Foundation of Sri Lanka*, **41**: 185–194.
- Ardolino, L. I., Meloni, M., Brugali, G., Corsini, E., & Galli, C. L. (2016) Preclinical evaluation of tolerability of a selective, bacteriostatic, locally active vaginal formulation. *Current Therapeutic Research, Clinical and Experimental*, **83**:13–21.
- Baâzaoui, M., Béjaoui, I., Kalfat, R., Amdouni, N., Hbaieb, S., & Chevalier, Y. (2016) Interfacial properties and thermodynamic behavior of cationic amphiphilic  $\beta$ -cyclodextrins substituted with one or seven alkyl chains. *RSC Advances*, **6**:72044–72054.
- Bálint, J., Egri, G., Kolbert, A., Dianóczy, C., Fogassy, E., Novák, L., & Poppe, L. (1999) Baker's yeast mediated reduction of dihydroxyacetone derivatives. *Tetrahedron: Asymmetry*, **10**: 4017–4028.
- Bayach, I., Manickam-Achary, V., Iskandar, W. F. N. W., Sugimura, A., & Hashim, R. (2016) Computational insights into octyl-D-xyloside isomers towards understanding the liquid crystal-line structure: Physico-chemical features. *Liquid Crystals*, **43**:1–11.
- Bouxin, F., Marinkovic, S., Bras, J. L., & Estrine, B. (2010) Direct conversion of xylan into alkyl pentosides. *Carbohydrate Research*, **345**:2469–2473.
- Charoensapayan, R., Ito, K., Rudeekulthamrong, P., & Kaulpiboon, J. (2016) Enzymatic synthesis of propyl- $\alpha$ -glycosides and their application as emulsifying and antibacterial agents. *Bio-technology and Bioprocess Engineering*, **21**:389–401.
- Chatron-Colliet, A., Brusa, C., Bertin-Jung, I., Gulberti, S., Ramalanjaona, N., Fournel-Gigleux, S., ... Wegrowski, Y. (2017) 'Click'-xylosides as initiators of the biosynthesis of glycosaminoglycans: Comparison of mono-xylosides with xylobiosides. *Chemical Biology & Drug Design*, **89**:319–326.
- Chen, G., Li, Z., Chen, L., Ji, S., & Shen, W. (2016) Synthesis and properties of alkyl  $\beta$ -D-galactopyranoside. *Journal of Surfactants and Detergents*, **19**:1095–1105.
- Chen, G., Li, Z., Chen, L., Ji, S., & Shen, W. (2017) Synthesis and properties of alkyl  $\alpha$ -D-galactopyranoside. *Journal of Dispersion Science and Technology*, **38**:506–514.
- Chen, L., & Kong, F. (2002) An efficient and practical synthesis of  $\beta$ -(1 $\rightarrow$ 3)-linked xylooligosaccharides. *Carbohydrate Research*, **337**:2335–2341.
- Chen, L., Shen, W. Z., Kuang, N., & Ji, S. W. (2016) Synthesis of hexadecyl  $\beta$ -D-xylopyranoside. *Journal of Xuzhou Institute of Technology (Natural Science Edition)*, **31**:10–14 (in Chinese).
- Damez, C., Bouquillon, S., Harakat, D., Hénin, F., Muzart, J., Pezron, I., & Komunjer, L. (2007) Alkenyl and alkenoyl amphiphilic derivatives of D-xylose and their surfactant properties. *Carbohydrate Research*, **342**:154–162.
- Das, M., Du, Y., Ribeiro, O., Hariharan, P., Mortensen, J. S., Patra, D., ... Chae, P. S. (2017) Conformationally preorganized diastereomeric norbornane-based maltosides for membrane protein study: Implications of detergent kink for micellar properties. *Journal of the American Chemical Society*, **139**:3072–3081.
- de Souza, J., Pontes, K., Alves, T., Amaral, V., Rebelo, M., Hausen, M., & Chaud, M. (2017) Spotlight on biomimetic systems based on lyotropic liquid crystal. *Molecules*, **22**:419.
- Du, Z., Wang, C., Tai, X., Wang, G., & Liu, X. (2016) Optimization and characterization of biocompatible oil-in-water nanoemulsion for pesticide delivery. *ACS Sustainable Chemistry & Engineering*, **4**:983–991.
- Eastoe, J., & Dalton, J. S. (2000) Dynamic surface tension and adsorption mechanisms of surfactants at the air-water interface. *Advances in Colloid and Interface Science*, **85**:103–144.
- El-Sukkary, M. M. A., Syed, N. A., Aiad, I., & El-Azab, W. I. M. (2008) Synthesis and characterization of some alkyl polyglycosides surfactants. *Journal of Surfactants and Detergents*, **11**:129–137.
- Fainerman, V. B., Kazakov, V. N., Lylyk, S. V., Makievski, A. V., & Miller, R. (2004) Dynamic surface tension measurements of surfactant solutions using the maximum bubble pressure method—Limits of applicability. *Colloids and Surfaces A: Physicochemical and Engineering Aspects*, **250**:97–102.
- Gao, Y., Yang, X., Bai, L., & Zhang, J. (2014) Preparation and physicochemical properties of disodium lauryl glucoside sulfosuccinate. *Journal of Surfactants and Detergents*, **17**:603–608.
- Geetha, D., & Tyagi, R. (2012) Alkyl poly glucosides (APGs) surfactants and their properties: A review. *Tenside, Surfactants, Detergents*, **49**:417–427.
- Guo, D. H., Xu, Y. S., Kang, Y. J., Han, S. Y., & Zheng, S. P. (2016) Synthesis of octyl- $\beta$ -D-glucopyranoside catalyzed by Thai rosewood  $\beta$ -glucosidase-displaying *Pichia pastoris* in an aqueous/organic two-phase system. *Enzyme and Microbial Technology*, **85**: 90–97.
- Han, Z., Yang, X., Liu, Y., Wang, J., & Gao, Y. (2015) Physicochemical properties and phase behavior of didecyltrimethylammonium chloride/alkyl polyglycoside surfactant mixtures. *Journal of Surfactants and Detergents*, **18**:641–649.
- Hashim, R., Mirzadeh, S. M., Heidelberg, T., Minamikawa, H., Yoshiaki, T., & Sugimura, A. (2011) A reevaluation of the epimeric and anomeric relationship of glucosides and galactosides in thermotropic liquid crystal self-assemblies. *Carbohydrate Research*, **346**: 2948–2956.



- Hashim, R., Sugimura, A., Minamikawa, H., & Heidelberg, T. (2012) Nature-like synthetic alkyl branched-chain glycolipids: A review on chemical structure and self-assembly properties. *Liquid Crystals*, **39**:1–17.
- Hong, E., Kim, J., Rhie, S., Ha, S. J., Kim, J., & Ryu, Y. (2016) Optimization of dilute sulfuric acid pretreatment of corn stover for enhanced xylose recovery and xylitol production. *Biotechnology and Bioengineering*, **21**:612–619.
- Kuang, N., Wu, G., Chen, L., Xia, S., Li, Z., Chen, G., & Ye, X. (2016) Synthesis and properties of alkyl  $\beta$ -D-xylopyranosides. *Journal of Central South University of Technology*, **47**:3323–3331 (in Chinese).
- Lagerwall, J. P. F., & Scalia, G. (2012) A new era for liquid crystal research: Applications of liquid crystals in soft matter nano-, bio- and microtechnology. *Current Applied Physics*, **12**:1387–1412.
- Li, L. J. (2007) Study on the determination of PAA solubility and the extraction technology. *Applied Chemical Industry*, **36**:547–549 (in Chinese).
- Li, Z., Chen, G., Chen, L., Shen, W., & Ji, S. (2016) Synthesis and properties of alkyl  $\alpha$ -D-glucopyranosides. *Chinese Journal of Applied Chemistry*, **33**:1265–1273 (in Chinese).
- Liew, C. Y., Salim, M., Zahid, N. I., & Hashim, R. (2015) Biomass derived xylose Guerbet surfactants: Thermotropic and lyotropic properties from small-angle X-ray scattering. *RSC Advances*, **120**: 99125–99132.
- Liu, D., Chen, L., Li, H., Zeng, S., Kuang, N., & Tian, J. (2013) Syntheses and properties of alkyl  $\beta$ -D-glucopyranosides. *Chinese Journal of Applied Chemistry*, **30**:1120–1126 (in Chinese).
- Lukic, M., Pantelic, I., & Savic, S. (2016) An overview of novel surfactants for formulation of cosmetics with certain emphasis on acidic active substances. *Tenside, Surfactants, Detergents*, **53**:7–19.
- Ochs, M., Muzard, M., Plantier-Royon, R., Estrine, B., & Rémond, C. (2011) Enzymatic synthesis of alkyl  $\beta$ -D-xylosides and oligoxylosides from xylans and from hydrothermally pretreated wheat bran. *Green Chemistry*, **13**:2380–2388.
- Oldham, E. D., Seelam, S., Lema, C., Aguilera, R. J., Fiegel, J., Rankin, S. E., ... Lehmler, H. J. (2013) Synthesis, surface properties, and biocompatibility of 1,2,3-triazole-containing alkyl  $\beta$ -D-xylopyranoside surfactants. *Carbohydrate Research*, **379**:68–77.
- Qian, S. Q., Zhou, L. F., Shi, Y. Z., Wu, Y. H., Xu, H., & Lu, Z. X. (2016) Sodium hydroxide-induced process for efficient xylan extraction from corn straws. *Current Topics in Nutraceutical Research*, **14**:73–80.
- Rather, M. Y., & Mishra, S. (2013)  $\beta$ -Glycosidases: An alternative enzyme based method for synthesis of alkyl-glycosides. *Sustainable Chemical Processes*, **1**:1–15.
- Reading, E., Liko, I., Allison, T. M., Benesch, J. L. P., Laganowsky, A., & Robinson, C. V. (2015) The role of the detergent micelle in preserving the structure of membrane proteins in the gas phase. *Angewandte Chemie, International Edition*, **54**: 4577–4581.
- Renault, B., Portella, C., Marinkovic, S., & Estrine, B. (2012) Synthesis and surface properties of succinic acid end-capped alkyl-polyxylosides. *Journal of Surfactants and Detergents*, **15**: 191–198.
- Renciuk, D., Blacque, O., Vorlickova, M., & Spingler, B. (2013) Crystal structures of B-DNA dodecamer containing the epigenetic modifications 5-hydroxymethylcytosine or 5-methylcytosine. *Nucleic Acids Research*, **41**:9891–9900.
- Ríos, F., Fernández-Arteaga, A., Lechuga, M., Jurado, E., & Fernández-Serrano, M. (2016) Kinetic study of the anaerobic biodegradation of alkyl polyglucosides and the influence of their structural parameters. *Environmental Science and Pollution Research*, **23**:8286–8293.
- Ruckenstein, E. (1996) Microemulsions, macroemulsions, and the Bancroft rule. *Langmuir*, **12**:6351–6353.
- Satgé, C., Bras, J. L., Hénin, F., & Muzart, J. (2005) DMF promoted xylosylation of terpenols. *Tetrahedron*, **61**:8405–8409.
- Sulek, M. W., Ogorzałek, M., Wasilewski, T., & Klimaszewska, E. (2013) Alkyl polyglucosides as components of water based lubricants. *Journal of Surfactants and Detergents*, **16**:369–375.
- Tardy-Planechaud, S., Fujimoto, J., Lin, S. S., & Sowers, L. C. (1997) Solid phase synthesis and restriction endonuclease cleavage of oligodeoxynucleotides containing 5-(hydroxymethyl)-cytosine. *Nucleic Acids Research*, **25**:553–559.
- Turner, P., Svensson, D., Adlercreutz, P., & Karlsson, E. (2007) A novel variant of *Thermotoga neapolitana*  $\beta$ -glucosidase B is an efficient catalyst for the synthesis of alkyl glucosides by transglycosylation. *Journal of Biotechnology*, **130**:67–74.
- von Rybinski, W., & Hill, K. (1998) Alkyl polyglucosides: Properties and applications of a new class of surfactants. *Angewandte Chemie, International Edition*, **37**:1328–1345.
- Weuthen, M., Kawa, R., Hill, K., & Ansmann, A. (1995) Long chain alkyl polyglucosides: A new generation of emulsifiers. *European Journal of Lipid Science and Technology*, **97**:209–211.
- Xu, W., Osei-Prempeh, G., Lema, C., Oldham, E. D., Aguilera, R. J., Parkin, S., ... Lehmler, H. J. (2012) Synthesis, thermal properties and cytotoxicity evaluation of hydrocarbon and fluorocarbon alkyl  $\beta$ -D-xylopyranoside surfactants. *Carbohydrate Research*, **349**: 12–23.
- Ying, G. Q., Yang, H., Yi, Y., & Xu, F. (2007) Relationships between the molecular structure and moisture-absorption and moisture-retention abilities of succinyl chitosan. *Polymer Bulletin*, **59**:509–516.
- Yuan, Y., Teng, Q., Zhong, R., & Ye, Z. (2015) TBL3 and TBL31, two Arabidopsis DUF231 domain proteins, are required for 3-O-monoacetylation of xylan. *Plant & Cell Physiology*, **57**:35–45.

## Biographies

**Wangzhen Shen** is a postgraduate student in college of chemistry at Xiangtan University. She obtained her B.E. in food quality and safety from Jishou University in 2014. Her studies involve the synthesis and application of sugar-based surfactants.

**Shanwei Ji** is a postgraduate student in college of chemistry at Xiangtan University. He obtained his B.Sc. in materials chemistry from Yulin Normal University in 2014. His studies involve the synthesis and application of alkyl glycoside.

**Langqiu Chen** received his B.Sc. in chemistry from Xiangtan University in 1984, his M.E. in food Engineering from Light Industry Institute of Tianjing in 1990, and his Ph.D. from the Graduate School of Chinese Academy of Sciences (Research Center for Eco-Environmental Science, Academia Sinica) in 2003. He worked as a guest researcher in Ryukoku University which was supported by JSPS for ten months and as a postdoctoral position in department of chemistry at Oxford University for one year. He is a professor in college of chemistry at Xiangtan University. His studies involve the research of carbohydrate chemistry, sugar-based surfactants, organic synthesis, pharmaceutical synthesis and food additives.

**Yanhua Zhang** is a postgraduate student in college of chemistry at Xiangtan University. She obtained his B.Sc. in chemistry from Hengyang Normal University in 2015. Her studies involve the synthesis and application of alkyl glycoside.

**Xiubing Wu** is a postgraduate student in college of chemistry at Xiangtan University. He obtained his B.E. in chemical engineering and technology from Hunan Institute of Engineering in 2016. His studies involve the synthesis and application of alkyl glycoside.